Observation of the decay $D^0 \to \omega\phi$

M. Ablikim[1], M. N. Achasov[10,c], P. Adlarson[67], S. Ahmed[15], M. Albrecht[4], R. Aliberti[28], A. Amoroso[66A,66C], M. R. An[32], Q. An[63,49], X. H. Bai[57], Y. Bai[48], O. Bakina[29], R. Baldini Ferroli[23A], I. Balossino[24A], Y. Ban[38,j], K. Begzsuren[26], N. Berger[28], M. Bertani[23A], D. Bettoni[24A], F. Bianchi[66A,66C], J. Bloms[60], A. Bortone[66A,66C], I. Boyko[29], R. A. Briere[5], H. Cai[68], X. Cai[1,49], A. Calcaterra[23A], G. F. Cao[1,54], N. Cao[1,54], S. A. Cetin[53A], J. F. Chang[1,49], W. L. Chang[1,54], G. Chelkov[29,b], D. Y. Chen[6], G. Chen[1], H. S. Chen[1,54], M. L. Chen[1,49], S. J. Chen[35], X. R. Chen[25], Y. B. Chen[1,49], Z. J Chen[20,k], W. S. Cheng[66C], G. Cibinetto[24A], F. Cossio[66C], X. F. Cui[36], H. L. Dai[1,49], X. C. Dai[1,54], A. Dbeyssi[15], R. E. de Boer[4], D. Dedovich[29], Z. Y. Deng[1], A. Denig[28], I. Denysenko[29], M. Destefanis[66A,66C], F. De Mori[66A,66C], Y. Ding[33], C. Dong[36], J. Dong[1,49], L. Y. Dong[1,54], M. Y. Dong[1,49,54], X. Dong[68], S. X. Du[71], Y. L. Fan[68], J. Fang[1,49], S. S. Fang[1,54], Y. Fang[1], R. Farinelli[24A], L. Fava[66B,66C], F. Feldbauer[4], G. Felici[23A], C. Q. Feng[63,49], J. H. Feng[50], M. Fritsch[4], C. D. Fu[1], Y. Gao[64], Y. Gao[38,j], Y. Gao[63,49], Y. G. Gao[6], I. Garzia[24A,24B], P. T. Ge[68], C. Geng[50], E. M. Gersabeck[58], A Gilman[61], K. Goetzen[11], L. Gong[33], W. X. Gong[1,49], W. Gradl[28], M. Greco[66A,66C], L. M. Gu[35], M. H. Gu[1,49], S. Gu[2], Y. T. Gu[13], C. Y Guan[1,54], A. Q. Guo[22], L. B. Guo[34], R. P. Guo[40], Y. P. Guo[9,h], A. Guskov[29,b], T. T. Han[41], W. Y. Han[32], X. Q. Hao[16], F. A. Harris[56], K. L. He[1,54], F. H. Heinsius[4], C. H. Heinz[28], T. Held[4], Y. K. Heng[1,49,54], C. Herold[51], M. Himmelreich[11,f], T. Holtmann[4], G. Y. Hou[1,54], Y. R. Hou[54], Z. L. Hou[1], H. M. Hu[1,54], J. F. Hu[47,l], T. Hu[1,49,54], Y. Hu[1], G. S. Huang[63,49], L. Q. Huang[64], X. T. Huang[41], Y. P. Huang[1], Z. Huang[38,j], T. Hussain[65], N Hüsken[22,28], W. Ikegami Andersson[67], W. Imoehl[22], M. Irshad[63,49], S. Jaeger[4], S. Janchiv[26], Q. Ji[1], Q. P. Ji[16], X. B. Ji[1,54], X. L. Ji[1,49], Y. Y. Ji[41], H. B. Jiang[41], X. S. Jiang[1,49,54], J. B. Jiao[41], Z. Jiao[18], S. Jin[35], Y. Jin[57], M. Q. Jing[1,54], T. Johansson[67], N. Kalantar-Nayestanaki[55], X. S. Kang[33], R. Kappert[55], M. Kavatsyuk[55], B. C. Ke[43,1], I. K. Keshk[4], A. Khoukaz[60], P. Kiese[28], R. Kiuchi[1], R. Kliemt[11], L. Koch[30], O. B. Kolcu[53A,e], B. Kopf[4], M. Kuemmel[4], M. Kuessner[4], A. Kupsc[67], M. G. Kurth[1,54], W. Kühn[30], J. J. Lane[58], J. S. Lange[30], P. Larin[15], A. Lavania[21], L. Lavezzi[66A,66C], Z. H. Lei[63,49], H. Leithoff[28], M. Lellmann[28], T. Lenz[28], C. Li[39], C. H. Li[32], Cheng Li[63,49], D. M. Li[71], F. Li[1,49], G. Li[1], H. Li[63,49], H. Li[43], H. B. Li[1,54], H. J. Li[16], J. L. Li[41], J. Q. Li[4], J. S. Li[50], Ke Li[1], L. K. Li[1], Lei Li[3], P. R. Li[31,m,n], S. Y. Li[52], W. D. Li[1,54], W. G. Li[1], X. H. Li[63,49], X. L. Li[41], Xiaoyu Li[1,54], Z. Y. Li[50], H. Liang[1,54], H. Liang[63,49], H. Liang[27], Y. F. Liang[45], Y. T. Liang[25], G. R. Liao[12], L. Z. Liao[1,54], J. Libby[21], C. X. Lin[50], B. J. Liu[1], C. X. Liu[1], D. Liu[15,63], F. H. Liu[44], Fang Liu[1], Feng Liu[6], H. B. Liu[13], H. M. Liu[1,54], Huanhuan Liu[1], Huihui Liu[17], J. B. Liu[63,49], J. L. Liu[64], J. Y. Liu[1,54], K. Liu[1], K. Y. Liu[33], L. Liu[63,49], M. H. Liu[9,h], P. L. Liu[1], Q. Liu[68], Q. Liu[54], S. B. Liu[63,49], Shuai Liu[46], T. Liu[1,54], W. M. Liu[63,49], X. Liu[31,m,n], Y. Liu[31,m,n], Y. B. Liu[36], Z. A. Liu[1,49,54], Z. Q. Liu[41], X. C. Lou[1,49,54], F. X. Lu[50], H. J. Lu[18], J. D. Lu[1,54], J. G. Lu[1,49], X. L. Lu[1], Y. Lu[1], Y. P. Lu[1,49], C. L. Luo[34], M. X. Luo[70], P. W. Luo[50], T. Luo[9,h], X. L. Luo[1,49], X. R. Lyu[54], F. C. Ma[33], H. L. Ma[1], L. L. Ma[41], M. M. Ma[1,54], Q. M. Ma[1], R. Q. Ma[1,54], R. T. Ma[54], X. X. Ma[1,54], X. Y. Ma[1,49], F. E. Maas[15], M. Maggiora[66A,66C], S. Maldaner[4], S. Malde[61], A. Mangoni[23B], Y. J. Mao[38,j], Z. P. Mao[1], S. Marcello[66A,66C], Z. X. Meng[57], J. G. Messchendorp[55], G. Mezzadri[24A], T. J. Min[35], R. E. Mitchell[22], X. H. Mo[1,49,54], Y. J. Mo[6], N. Yu. Muchnoi[10,c], H. Muramatsu[59], S. Nakhoul[11,f], Y. Nefedov[29], F. Nerling[11,f], I. B. Nikolaev[10,c], Z. Ning[1,49], S. Nisar[8,i], S. L. Olsen[54], Q. Ouyang[1,49,54], S. Pacetti[23B,23C], X. Pan[9,h], Y. Pan[58], A. Pathak[1], P. Patteri[23A], M. Pelizaeus[4], H. P. Peng[63,49], K. Peters[11,f], J. Pettersson[67], J. L. Ping[34], R. G. Ping[1,54], S. Pogodin[29], R. Poling[59], V. Prasad[63,49], H. Qi[63,49], H. R. Qi[52], K. H. Qi[25], M. Qi[35], T. Y. Qi[9], S. Qian[1,49], W. B. Qian[54], Z. Qian[50], C. F. Qiao[54], L. Q. Qin[12], X. P. Qin[9], X. S. Qin[41], Z. H. Qin[1,49], J. F. Qiu[1], S. Q. Qu[36], K. H. Rashid[65], K. Ravindran[21], C. F. Redmer[28], A. Rivetti[66C], V. Rodin[55], M. Rolo[66C], G. Rong[1,54], Ch. Rosner[15], M. Rump[60], H. S. Sang[63], A. Sarantsev[29,d], Y. Schelhaas[28], C. Schnier[4], K. Schoenning[67], M. Scodeggio[24A,24B], D. C. Shan[46], W. Shan[19], X. Y. Shan[63,49], J. F. Shangguan[46], M. Shao[63,49], C. P. Shen[9], H. F. Shen[1,54], P. X. Shen[36], X. Y. Shen[1,54], H. C. Shi[63,49], R. S. Shi[1,54], X. Shi[1,49], X D Shi[63,49], J. J. Song[41], W. M. Song[27,1], Y. X. Song[38,j], S. Sosio[66A,66C], S. Spataro[66A,66C], K. X. Su[68], P. P. Su[46], F. F. Sui[41], G. X. Sun[1], H. K. Sun[1], J. F. Sun[16], L. Sun[68], S. S. Sun[1,54], T. Sun[1,54], W. Y. Sun[34], W. Y. Sun[27], X Sun[20,k], Y. J. Sun[63,49], Y. K. Sun[63,49], Y. Z. Sun[1], Z. T. Sun[1], Y. H. Tan[68], Y. X. Tan[63,49], C. J. Tang[45], G. Y. Tang[1], J. Tang[50], J. X. Teng[63,49], V. Thoren[67], W. H. Tian[43], Y. T. Tian[25], I. Uman[53B], B. Wang[1], C. W. Wang[35], D. Y. Wang[38,j], H. J. Wang[31,m,n], H. P. Wang[1,54], K. Wang[1,49], L. L. Wang[1], M. Wang[41], M. Z. Wang[38,j], Meng Wang[1,54], W. Wang[50], W. H. Wang[68], W. P. Wang[63,49], X. Wang[38,j], X. F. Wang[31,m,n], X. L. Wang[9,h], Y. Wang[50], Y. Wang[63,49], Y. D. Wang[37], Y. F. Wang[1,49,54], Y. Q. Wang[1], Y. Y. Wang[31,m,n], Z. Wang[1,49], Z. Y. Wang[1], Ziyi Wang[54], Zongyuan Wang[1,54], D. H. Wei[12], F. Weidner[60], S. P. Wen[1], D. J. White[58], U. Wiedner[4], G. Wilkinson[61], M. Wolke[67], L. Wollenberg[4], J. F. Wu[1,54], L. H. Wu[1], L. J. Wu[1,54], X. Wu[9,h], Z. Wu[1,49], L. Xia[63,49], H. Xiao[9,h], S. Y. Xiao[1], Z. J. Xiao[34], X. H. Xie[38,j], Y. G. Xie[1,49], Y. H. Xie[6], T. Y. Xing[1,54], G. F. Xu[1], Q. J. Xu[14], W. Xu[1,54], X. P. Xu[46], Y. C. Xu[54], F. Yan[9,h], L. Yan[9,h], W. B. Yan[63,49], W. C. Yan[71], Xu Yan[46], H. J. Yang[42,g], H. X. Yang[1], L. Yang[43], S. L. Yang[54], Y. X. Yang[12], Yifan Yang[1,54], Zhi Yang[25], M. Ye[1,49], M. H. Ye[7], J. H. Yin[1], Z. Y. You[50], B. X. Yu[1,49,54], C. X. Yu[36], G. Yu[1,54], J. S. Yu[20,k], T. Yu[64], C. Z. Yuan[1,54], L. Yuan[2], X. Q. Yuan[38,j], Y. Yuan[1], Z. Y. Yuan[50], C. X. Yue[32], A. Yuncu[53A,a], A. A. Zafar[65], Zeng[6], Y. Zeng[20,k], A. Q. Zhang[1], B. X. Zhang[1], Guangyi Zhang[16], H. Zhang[63], H. H. Zhang[27], H. H. Zhang[50], H. Y. Zhang[1,49], J. J. Zhang[43], J. L. Zhang[69], J. Q. Zhang[34], J. W. Zhang[1,49,54], J. Y. Zhang[1], J. Z. Zhang[1,54], Jianyu Zhang[1,54], Jiawei Zhang[1,54], L. M. Zhang[52], L. Q. Zhang[50], Lei Zhang[35], S. Zhang[50], S. F. Zhang[35], Shulei Zhang[20,k], X. D. Zhang[37], X. Y. Zhang[41], Y. Zhang[61], Y. H. Zhang[1,49], Y. T. Zhang[63,49], Yan Zhang[63,49], Yao Zhang[1], Z. H. Zhang[6], Z. Y. Zhang[68], G. Zhao[1], J. Zhao[32], J. Y. Zhao[1,54], J. Z. Zhao[1,49], Lei Zhao[63,49], Ling Zhao[1], M. G. Zhao[36], Q. Zhao[1], S. J. Zhao[71], Y. B. Zhao[1,49], Y. X. Zhao[25], Z. G. Zhao[63,49], A. Zhemchugov[29,b], B. Zheng[64], J. P. Zheng[1,49], Y. Zheng[38,j], Y. H. Zheng[54], B. Zhong[34], C. Zhong[64], L. P. Zhou[1,54], Q. Zhou[1,54], X. Zhou[68], X. K. Zhou[54], X. R. Zhou[63,49], X. Y. Zhou[32], A. N. Zhu[1,54], J. Zhu[36], K. Zhu[1], K. J. Zhu[1,49,54], S. H. Zhu[62], T. J. Zhu[69], W. J. Zhu[9,h], W. J. Zhu[36], Y. C. Zhu[63,49], Z. A. Zhu[1,54], B. S. Zou[1], J. H. Zou[1]

(BESIII Collaboration)

[1] Institute of High Energy Physics, Beijing 100049, People's Republic of China
[2] Beihang University, Beijing 100191, People's Republic of China
[3] Beijing Institute of Petrochemical Technology, Beijing 102617, People's Republic of China
[4] Bochum Ruhr-University, D-44780 Bochum, Germany
[5] Carnegie Mellon University, Pittsburgh, Pennsylvania 15213, USA
[6] Central China Normal University, Wuhan 430079, People's Republic of China
[7] China Center of Advanced Science and Technology, Beijing 100190, People's Republic of China
[8] COMSATS University Islamabad, Lahore Campus, Defence Road, Off Raiwind Road, 54000 Lahore, Pakistan
[9] Fudan University, Shanghai 200443, People's Republic of China
[10] G.I. Budker Institute of Nuclear Physics SB RAS (BINP), Novosibirsk 630090, Russia
[11] GSI Helmholtzcentre for Heavy Ion Research GmbH, D-64291 Darmstadt, Germany
[12] Guangxi Normal University, Guilin 541004, People's Republic of China
[13] Guangxi University, Nanning 530004, People's Republic of China
[14] Hangzhou Normal University, Hangzhou 310036, People's Republic of China
[15] Helmholtz Institute Mainz, Staudinger Weg 18, D-55099 Mainz, Germany
[16] Henan Normal University, Xinxiang 453007, People's Republic of China
[17] Henan University of Science and Technology, Luoyang 471003, People's Republic of China
[18] Huangshan College, Huangshan 245000, People's Republic of China
[19] Hunan Normal University, Changsha 410081, People's Republic of China
[20] Hunan University, Changsha 410082, People's Republic of China
[21] Indian Institute of Technology Madras, Chennai 600036, India
[22] Indiana University, Bloomington, Indiana 47405, USA
[23] INFN Laboratori Nazionali di Frascati , (A)INFN Laboratori Nazionali di Frascati, I-00044, Frascati, Italy; (B)INFN Sezione di Perugia, I-06100, Perugia, Italy; (C)University of Perugia, I-06100, Perugia, Italy
[24] INFN Sezione di Ferrara, (A)INFN Sezione di Ferrara, I-44122, Ferrara, Italy; (B)University of Ferrara, I-44122, Ferrara, Italy
[25] Institute of Modern Physics, Lanzhou 730000, People's Republic of China
[26] Institute of Physics and Technology, Peace Ave. 54B, Ulaanbaatar 13330, Mongolia
[27] Jilin University, Changchun 130012, People's Republic of China
[28] Johannes Gutenberg University of Mainz, Johann-Joachim-Becher-Weg 45, D-55099 Mainz, Germany
[29] Joint Institute for Nuclear Research, 141980 Dubna, Moscow region, Russia
[30] Justus-Liebig-Universitaet Giessen, II. Physikalisches Institut, Heinrich-Buff-Ring 16, D-35392 Giessen, Germany
[31] Lanzhou University, Lanzhou 730000, People's Republic of China
[32] Liaoning Normal University, Dalian 116029, People's Republic of China
[33] Liaoning University, Shenyang 110036, People's Republic of China
[34] Nanjing Normal University, Nanjing 210023, People's Republic of China
[35] Nanjing University, Nanjing 210093, People's Republic of China
[36] Nankai University, Tianjin 300071, People's Republic of China
[37] North China Electric Power University, Beijing 102206, People's Republic of China
[38] Peking University, Beijing 100871, People's Republic of China
[39] Qufu Normal University, Qufu 273165, People's Republic of China
[40] Shandong Normal University, Jinan 250014, People's Republic of China
[41] Shandong University, Jinan 250100, People's Republic of China
[42] Shanghai Jiao Tong University, Shanghai 200240, People's Republic of China
[43] Shanxi Normal University, Linfen 041004, People's Republic of China
[44] Shanxi University, Taiyuan 030006, People's Republic of China
[45] Sichuan University, Chengdu 610064, People's Republic of China
[46] Soochow University, Suzhou 215006, People's Republic of China
[47] South China Normal University, Guangzhou 510006, People's Republic of China
[48] Southeast University, Nanjing 211100, People's Republic of China
[49] State Key Laboratory of Particle Detection and Electronics, Beijing 100049, Hefei 230026, People's Republic of China
[50] Sun Yat-Sen University, Guangzhou 510275, People's Republic of China
[51] Suranaree University of Technology, University Avenue 111, Nakhon Ratchasima 30000, Thailand
[52] Tsinghua University, Beijing 100084, People's Republic of China
[53] Turkish Accelerator Center Particle Factory Group, (A)Istanbul Bilgi University, 34060 Eyup, Istanbul, Turkey; (B)Near East University, Nicosia, North Cyprus, Mersin 10, Turkey
[54] University of Chinese Academy of Sciences, Beijing 100049, People's Republic of China
[55] University of Groningen, NL-9747 AA Groningen, The Netherlands
[56] University of Hawaii, Honolulu, Hawaii 96822, USA
[57] University of Jinan, Jinan 250022, People's Republic of China
[58] University of Manchester, Oxford Road, Manchester, M13 9PL, United Kingdom
[59] University of Minnesota, Minneapolis, Minnesota 55455, USA

[60] University of Muenster, Wilhelm-Klemm-Str. 9, 48149 Muenster, Germany
[61] University of Oxford, Keble Rd, Oxford, UK OX13RH
[62] University of Science and Technology Liaoning, Anshan 114051, People's Republic of China
[63] University of Science and Technology of China, Hefei 230026, People's Republic of China
[64] University of South China, Hengyang 421001, People's Republic of China
[65] University of the Punjab, Lahore-54590, Pakistan
[66] University of Turin and INFN, (A)University of Turin, I-10125, Turin, Italy; (B)University of Eastern Piedmont, I-15121, Alessandria, Italy; (C)INFN, I-10125, Turin, Italy
[67] Uppsala University, Box 516, SE-75120 Uppsala, Sweden
[68] Wuhan University, Wuhan 430072, People's Republic of China
[69] Xinyang Normal University, Xinyang 464000, People's Republic of China
[70] Zhejiang University, Hangzhou 310027, People's Republic of China
[71] Zhengzhou University, Zhengzhou 450001, People's Republic of China

[a] Also at Bogazici University, 34342 Istanbul, Turkey
[b] Also at the Moscow Institute of Physics and Technology, Moscow 141700, Russia
[c] Also at the Novosibirsk State University, Novosibirsk, 630090, Russia
[d] Also at the NRC "Kurchatov Institute", PNPI, 188300, Gatchina, Russia
[e] Also at Istanbul Arel University, 34295 Istanbul, Turkey
[f] Also at Goethe University Frankfurt, 60323 Frankfurt am Main, Germany
[g] Also at Key Laboratory for Particle Physics, Astrophysics and Cosmology, Ministry of Education; Shanghai Key Laboratory for Particle Physics and Cosmology; Institute of Nuclear and Particle Physics, Shanghai 200240, People's Republic of China
[h] Also at Key Laboratory of Nuclear Physics and Ion-beam Application (MOE) and Institute of Modern Physics, Fudan University, Shanghai 200443, People's Republic of China
[i] Also at Harvard University, Department of Physics, Cambridge, MA, 02138, USA
[j] Also at State Key Laboratory of Nuclear Physics and Technology, Peking University, Beijing 100871, People's Republic of China
[k] Also at School of Physics and Electronics, Hunan University, Changsha 410082, China
[l] Also at Guangdong Provincial Key Laboratory of Nuclear Science, Institute of Quantum Matter, South China Normal University, Guangzhou 510006, China
[m] Also at Frontiers Science Center for Rare Isotopes, Lanzhou University, Lanzhou 730000, People's Republic of China
[n] Also at Lanzhou Center for Theoretical Physics, Lanzhou University, Lanzhou 730000, People's Republic of China

Using a data sample corresponding to an integrated luminosity of 2.93 fb^{-1} collected at a center-of-mass energy $\sqrt{s} = 3.773$ GeV by the BESIII detector, the decay $D^0 \to \omega\phi$ is observed for the first time. The branching fraction is measured to be $(6.48 \pm 0.96 \pm 0.38) \times 10^{-4}$ with a significance of 6.3σ, where the first and second uncertainties are statistical and systematic, respectively. An angular analysis reveals that the ϕ and ω mesons from the $D^0 \to \omega\phi$ decay are transversely polarized.

Comprehensive studies of D meson decays into a pair of vector mesons (V) provide crucial information to test different theoretical models [1–3], measure CP-violating parameters and strong phases [4, 5], and understand the dynamics of $D^0 - \bar{D}^0$ mixing [6–8]. In particular, the polarization of vector mesons in D decays is an essential measurement to reveal its decay mechanism. The two vector mesons in $D^0 \to VV$ decay are produced in three polarization states corresponding to one longitudinal (H_0) and two transverse ($H_\pm$) partial-wave amplitudes, where the longitudinal amplitude is CP-even, and the transverse amplitudes are superpositions of CP-even and CP-odd states. Throughout this Letter, the charge-conjugate modes are always implied. Naïvely, factorization models predict that the longitudinal and transverse polarizations are comparable in $D^0 \to VV$ decays [7]. However, a previous measurement reveals that the decay $D^0 \to K^{*0}\rho^0$ appears to be completely transversely polarized [9, 10], which is contrary to the case of $B \to \rho\rho$ [11] and $D^0 \to \rho^0\rho^0$ decays [12] where longitudinal polarization dominates.

Until now, $D^0 \to VV$ decays have not been well explored and the polarization state of the resulting vector mesons is not known. The singly-Cabibbo-suppressed decay $D^0 \to \omega\phi$ can occur via internal emission of a W^+ boson, and its branching fraction (BF) is predicted to be $(0.023 - 0.072)\%$ by factorization approaches [1, 7], 0.35×10^{-4} assuming SU(3) symmetry with nonet symmetry [1], $(1.41 \pm 0.09) \times 10^{-3}$ by a factorization-assisted topological amplitude method [8], and $(0.011 - 0.036)\%$ by a heavy-quark effective Lagrangian and chiral perturbation theory [13]. To date, no signal for $D^0 \to \omega\phi$ has been observed experimentally, and only an upper limit on the BF, $\mathcal{B}(D^0 \to \omega\phi) < 2.1 \times 10^{-3}$ [14], is available.

The angular distributions of $D^0 \to VV$ are sensitive to spin correlations and final state interactions [15, 16]. In this analysis, we consider the decay $D^0 \to \omega\phi$ with the subsequent decays $\omega \to \pi^+\pi^-\pi^0$ and $\phi \to K^+K^-$, as shown in Fig. 1. The angular distribution is given by

$$\frac{1}{\Gamma}\frac{d^2\Gamma}{d\cos\theta_\omega d\cos\theta_K} = \frac{9}{4}\{\frac{1}{4}(1-f_L)\sin^2\theta_\omega \sin^2\theta_K + f_L \cos^2\theta_\omega \cos^2\theta_K\}, \quad (1)$$

where $f_L = H_0^2/(H_0^2 + H_-^2 + H_+^2)$ is the longitudinal polarization fraction, θ_ω is the angle between $\mathbf{p}^\omega_{\pi^+} \times \mathbf{p}^\omega_{\pi^-}$ and $-\mathbf{p}^\omega_{D^0}$ in the ω rest frame, and θ_K is the angle between $\mathbf{p}^\phi_{K^-}$ and $-\mathbf{p}^\phi_{D^0}$ in the ϕ rest frame. Here, $\mathbf{p}^\omega_{\pi^+}$, $\mathbf{p}^\omega_{\pi^-}$, $\mathbf{p}^\phi_{K^-}$, and $\mathbf{p}^{\omega/\phi}_{D^0}$ are the momenta of the π^+, π^-, K^- and D^0, respectively, in the rest frame of either the ω or ϕ meson. By integrating over $\cos\theta_\omega$ or $\cos\theta_K$ from -1 to $+1$, Eq. (1) is simplified to

$$\frac{1}{\Gamma}\frac{d\Gamma}{d\cos\theta} = \frac{3}{2}\{\frac{1}{2}(1-f_L)\sin^2\theta + f_L\cos^2\theta\}, \quad (2)$$

where θ can be either θ_ω or θ_K.

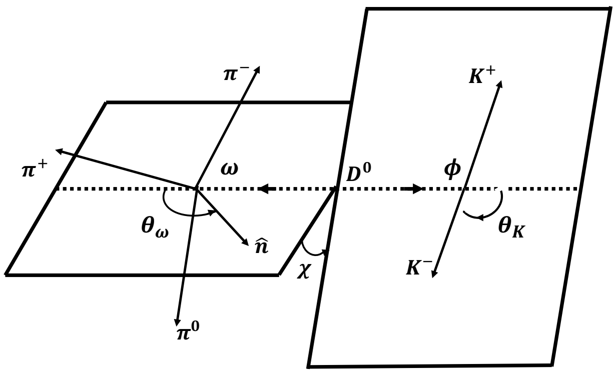

FIG. 1. The decay topology of $D^0 \to \omega\phi$ and the definitions of the decay angles.

In this Letter, we present the first measurement of $D^0 \to \omega\phi$ using a $\psi(3770)$ data sample corresponding to an integrated luminosity of 2.93 fb^{-1} collected by the BESIII detector [17]. The measurement is performed using the single-tag technique, where only one D^0 meson in the $\psi(3770) \to D^0\bar{D}^0$ decays is reconstructed in the mode of interest. Thus, the BF of $D^0 \to \omega\phi$ is calculated using

$$\mathcal{B} = \frac{N_{\rm sig}}{2 \cdot N_{D^0\bar{D}^0} \cdot \epsilon \cdot \mathcal{B}_{\rm sub}}, \quad (3)$$

where $N_{\rm sig}$ is the signal yield extracted from data, $N_{D^0\bar{D}^0} = (10597 \pm 28 \pm 89) \times 10^3$ is the total number of $\psi(3770) \to D^0\bar{D}^0$ decays [18], ϵ is the detection efficiency, and $\mathcal{B}_{\rm sub}$ is the product of BFs for the intermediate-state decays.

A detailed description of the design and performance of the BESIII detector can be found in Ref. [19]. A Monte Carlo (MC) simulation tool based on GEANT4 [20] is implemented, in which the e^+e^- annihilation is simulated with the KKMC generator [21] incorporating the effects of beam-energy spread and initial-state-radiation (ISR). An inclusive MC sample, composed of $D\bar{D}$ and non-$D\bar{D}$ events, ISR production of both $\psi(3686)$ and J/ψ, and continuum processes $e^+e^- \to q\bar{q}$ ($q = u, d, s$), is used to study the potential background. In the MC sample, the known decay modes are generated with EVTGEN [22] using BFs from the Particle Data Group (PDG) [23], and the remaining unknown decays are generated with LUNDCHARM [24]. The signal sample of $D^0 \to \phi\omega$ decays is modeled by a scalar meson decaying into two vector mesons with transverse polarization using EVTGEN [22].

The ϕ and ω candidates are reconstructed from their dominant decays $\phi \to K^+K^-$ and $\omega \to \pi^+\pi^-\pi^0$, respectively, where the π^0 is identified by a photon pair. The charged tracks must be within the main drift chamber (MDC) acceptance region by requiring the polar angle $|\cos\theta| < 0.93$, and must originate from the interaction point (IP) with a distance of closest approach within ± 1 cm in the plane perpendicular to the beam and ± 10 cm along the beam direction. Particle identification (PID) is performed by requiring $\mathcal{L}_\pi > \mathcal{L}_K$ and $\mathcal{L}_K > \mathcal{L}_\pi$ for the $\pi^\pm$ and $K^\pm$ candidates, respectively, where $\mathcal{L}_\pi$ and $\mathcal{L}_K$ are the likelihoods for the pion and kaon hypotheses calculated by combining the time-of-flight (TOF) information from the TOF detector and the dE/dx information from the MDC.

Photon candidates are selected from neutral showers deposited in the electromagnetic calorimeter (EMC) with energies larger than 25 MeV in the barrel region ($|\cos\theta| < 0.80$) and 50 MeV in the end-cap regions ($0.86 < |\cos\theta| < 0.92$). The EMC timing is required to be within 700 ns relative to the event start time to suppress electronic noise and deposited energy unrelated to the collision events. Furthermore, a photon candidate is required to be at least 10° away from any charged tracks to avoid any overlap between them. A π^0 candidate is formed by a photon pair with invariant mass within $(0.115, 0.150)$ GeV/c^2. To improve the resolution, a kinematic fit is imposed on the selected photon pair by constraining their invariant mass at the nominal π^0 mass [23], and the resultant kinematic variables are used in the subsequent analysis.

To identify the D^0 signal, the energy difference $\Delta E = E_D - E_{\rm beam}$ and the beam-constrained mass $M_{\rm BC} = \sqrt{E^2_{\rm beam}/c^4 - p^2_D/c^2}$ are calculated, where $E_{\rm beam}$ is the beam energy, and E_D (p_D) is the reconstructed energy (momentum) of the D^0 candidate in the e^+e^- center-of-mass system. The D^0 signal peaks around zero in the ΔE distribution and around the nominal D^0 mass (m_D) in the $M_{\rm BC}$ distribution. The $D^0 \to \omega\phi$ signal is reconstructed from all possible $\pi^+\pi^-\pi^0K^+K^-$ combinations. If there is more than one combination, the one with a minimum value of $|\Delta E|$ is selected. A D^0 candidate is required to satisfy $M_{\rm BC} > 1.84$ GeV/c^2 and $-0.03 < \Delta E < 0.02$ GeV. The ΔE requirement corresponds to an interval of 4 standard deviations from the peak position. The asymmetric boundaries stem from the photon energy detection in the EMC. A prominent peak corresponding to the K^0_S in the $M_{\pi^+\pi^-}$ distribution, arising from the background process $D^0 \to K^0_S +$ anything, is rejected by removing the mass range $(0.490, 0.503)$ GeV/c^2.

Figure 2 shows the $M_{\rm BC}$ distribution for the survived events of data and the background predictions from various MC samples with the K^+K^- invariant mass $M_{K^+K^-} < 1.05$ GeV/c^2 and the $\pi^+\pi^-\pi^0$ invariant mass $M_{\pi^+\pi^-\pi^0} > 0.65$ GeV/c^2, where the clear peak around m_D in data refers to the signal of $D^0 \to \pi^+\pi^-\pi^0K^+K^-$.

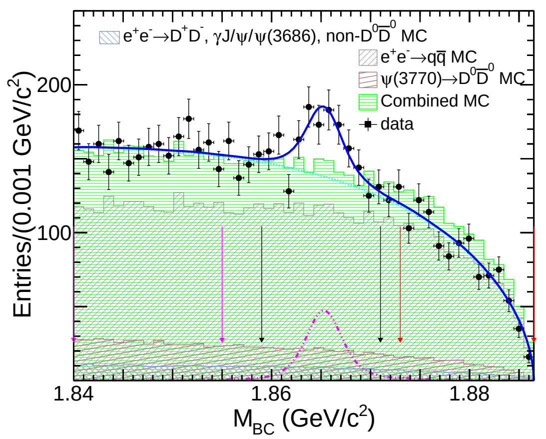

FIG. 2. Fit to the $M_{\rm BC}$ distribution of the candidate events for $D^0 \to \pi^+\pi^-\pi^0K^+K^-$. Black dots with error bars are data, dashed cyan curve for combinatorial background, long dashed-dotted pink curve for the D^0 signal, the solid blue curve for the total fit, and shadow histograms for the non-D^0 background predictions from various MC samples. The two black and two pink (red) arrows represent the $M_{\rm BC}$ signal and low (high)-sideband regions, respectively.

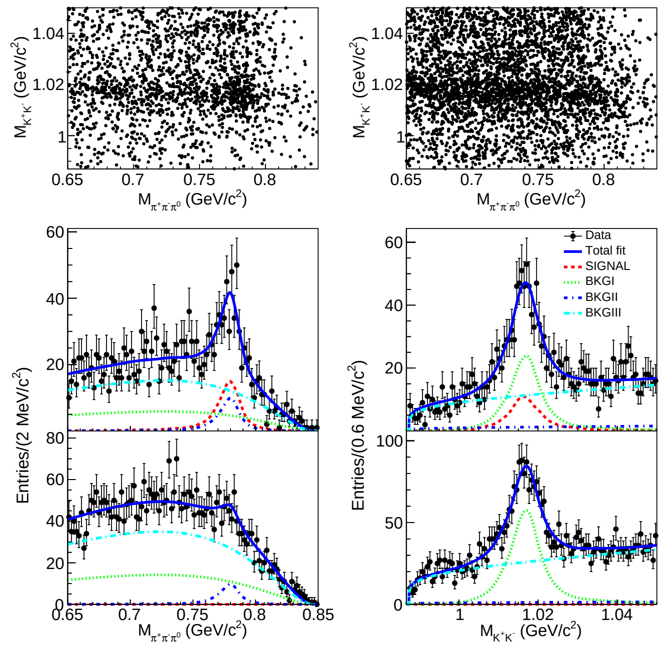

FIG. 3. (Top) the distributions of $M_{K^+K^-}$ versus $M_{\pi^+\pi^-\pi^0}$ in the $M_{\rm BC}$ signal (left) and sideband (right) regions, and (middle and bottom) the corresponding 1-D projection plots of $M_{\pi^+\pi^-\pi^0}$ (left) and $M_{K^+K^-}$ (right). The middle and bottom plots are produced in the $M_{\rm BC}$ signal and sideband regions, respectively. In the projection plots, the black dots with error bars are data, the solid blue, dashed red, dotted green, dashed-dotted blue, and long dashed-dotted cyan curves represent total fit results, SIGNAL, BKGI, BKGII, and BKGIII, respectively.

The $D^0 \to \omega\phi$ signal is evident in Fig. 3, where the distribution of $M_{\pi^+\pi^-\pi^0}$ versus $M_{K^+K^-}$ as well as their corresponding projection plots are shown for events in the $M_{\rm BC}$ signal region $(1.859, 1.871)$ GeV/c^2 and sideband region $(1.840, 1.855) \cup (1.873, 1.890)$ GeV/c^2. A cluster of events around the intersection of the ω and ϕ nominal masses in the $M_{\rm BC}$ signal region indicates the signal $D^0 \to \omega\phi$. There is no corresponding cluster of events in the sideband plot. Clear ϕ signal events are observed in the $M_{\rm BC}$ sideband region, indicating the contribution of the ϕ meson from non-D^0 decays. Prominent ω signal events are present in the $M_{\rm BC}$ signal region but absent in the corresponding sideband region, indicating the contribution of the ω meson from D^0 decays.

To extract the signal yield, a two-dimensional (2D) unbinned maximum likelihood fit is performed on the $M_{\pi^+\pi^-\pi^0}$ versus $M_{K^+K^-}$ distributions. This fit is performed simultaneously in both the $M_{\rm BC}$ signal and sideband regions, where the sideband events are used to constrain the background from non-D^0 decays. The fit includes a signal component, SIGNAL, which has both ω and ϕ intermediate states, and three backgrounds, BKGI, BKGII, and BKGIII. The BKGI (BKGII) contains only the ω (ϕ) intermediate state, and BKGIII includes neither the ω nor ϕ intermediate states. It is worth noting that the above four components may exist in both D^0 and non-D^0 decays. The yield of the signal $D^0 \to \omega\phi$ is extracted from the $M_{\rm BC}$ signal region by subtracting the contribution from non-D^0 decays estimated from the $M_{\rm BC}$ sideband region.

The SIGNAL is described by a distribution obtained from a 2D kernel estimation [25] of the unbinned signal MC samples. BKGI is parameterized with the product of a distribution obtained from a 1D kernel estimation [25] of the ω signal MC for the $M_{\pi^+\pi^-\pi^0}$ distribution and a reversed ARGUS function [26] defined by the formula of Eq.(4) in Ref. [27] for the $M_{K^+K^-}$ distribution. Vice versa, BKGII is described with the product of an ARGUS function for the $M_{\pi^+\pi^-\pi^0}$ distribution and a distribution obtained from a 1D kernel estimation of the ϕ signal MC for the $M_{K^+K^-}$ distribution. BKGIII is the product of an ARGUS function for the $M_{\pi^+\pi^-\pi^0}$ distribution and a reversed ARGUS function for the $M_{K^+K^-}$ distribution. To compensate for the resolution difference between data and simulation, the shapes derived from simulation are convolved with (1D or 2D) Gaussian functions, which share the same parameters between different fit components and these parameters are floated during the fit. The endpoints of the ARGUS functions are fixed to the corresponding threshold values of $(m_D - m_\phi)$ and $2m_{K^\pm}$, respectively, where m_ϕ $(m_{K^\pm})$ is the nominal mass of the ϕ $(K^\pm)$ meson [23].

Detailed MC studies show that the non-peaking background shapes in the $M_{K^+K^-}$ distributions are identical in both the $M_{\rm BC}$ signal and sideband regions, but slightly different for $M_{\pi^+\pi^-\pi^0}$ distributions due to the threshold effect of kinematics. Thus, the reversed ARGUS parameterizations of the $M_{K^+K^-}$ distributions share the same parameters in both $M_{\rm BC}$ signal and sideband regions, but no constraint is implemented for the ARGUS functions for the $M_{\pi^+\pi^-\pi^0}$ distributions in different $M_{\rm BC}$ regions. We float SIGNAL, BKGI, BKGII, and BKGIII components in both $M_{\rm BC}$ signal and sideband regions during the fit. The final signal yield is also constrained to be $N_{\rm SG} = N_{\rm sig} + f \cdot N_{\rm SB}$, where $N_{\rm SG}$ and $N_{\rm SB}$ are the numbers of the SIGNAL component in the $M_{\rm BC}$ signal and sideband regions, respectively, as shown in Fig. 3. The factor f is the ratio of the corresponding yields from the non-D^0 decay in the $M_{\rm BC}$ signal and sideband regions, and its value is determined to be $(44.3 \pm 0.9)\%$ by fitting the $M_{\rm BC}$ distribution, as shown in Fig. 2. In this fit, the D^0 signal is described by the simulated signal shape convolved with a Gaussian function while the non-D^0 background by an ARGUS function [26]. The 2D simultaneous fit yields $N_{\rm sig} = 195.9 \pm 29.1$, which includes the uncertainties from $N_{\rm SB}$ and $N_{\rm SG}$. The detection efficiency is calculated to be $(3.32 \pm 0.04)\%$ by the same 2D simultaneous fit approach with an inclusive MC sample, which is a mixture of the signal MC sample generated by considering the polarization of $D^0 \to \omega\phi$ as discussed below, and various backgrounds. The BF of $D^0 \to \omega\phi$ is determined to be $(6.48 \pm 0.96 \pm 0.38) \times 10^{-4}$ according to Eq. (3), where the first and second uncertainties are statistical and systematic, respectively. The corresponding significance is 6.3 σ calculated by $\sqrt{-2\ln(\mathcal{L}_0/\mathcal{L}_{\rm max})}$ including both statistical and systematic unncertainties, where $\mathcal{L}_{\rm max}$ and $\mathcal{L}_0$ are the likelihood values for the nominal fit and the alternative fit with zero signal assumption, respectively. Different contributions to the systematic uncertainty will be described later.

To study the polarization in the $D^0 \to \omega\phi$ decay, the efficiency-corrected signal yields are evaluated in five equal bins of $|\cos\theta_\omega|$ and $|\cos\theta_K|$ as shown in Fig. 4. Here, we extract the signal yield in each bin using a procedure similar to the 2D simultaneous fit approach discussed above. The corresponding detection efficiency is obtained using a simulated signal sample generated uniformly over phase space (PHSP). A joint χ^2 fit on the $|\cos\theta_\omega|$ and $|\cos\theta_K|$ distributions of data is performed with Eq. (2), where f_L is floated between $[-1, 1]$. The fit yields $f_L = 0.00 \pm 0.10 \pm 0.08$, which corresponds to $f_L < 0.24$ at 95% confidence level computed by integrating the likelihood versus f_L curve from zero to 95% of the total curve after including the systematic uncertainty as described below. This result indicates that the vector mesons are transversely polarized in the $D^0 \to \omega\phi$ decay.

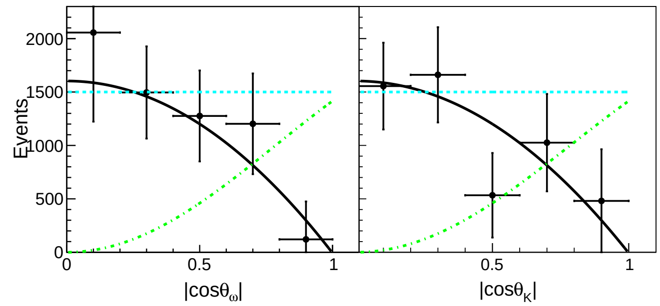

FIG. 4. The distribution of the background-subtracted signal yield corrected by the efficiency versus $|\cos\theta_\omega|$ (left) and $|\cos\theta_K|$ (right). The black dots with error bars are data with both statistical and systematic uncertainties, and the solid black curves are the fit results. The distributions with the longitudinal polarization and PHSP assumptions are shown as the dotted dashed green and dashed cyan curves, respectively.

According to Eq. (3), the systematic uncertainties for the BF measurement include those from the reconstruction efficiency, MC modeling, signal yield, number of $D^0\bar{D}^0$ events, and the BFs of the intermediate-state decays. The uncertainties associated with the reconstruction efficiency include tracking and PID of the charged tracks, π^0 reconstruction, ΔE requirement, and K^0_S veto.

The uncertainty associated with the tracking efficiency is studied using a control sample of $\psi(3770) \to D\bar{D}$ with hadronic D decays via a partial reconstruction method [28, 29], where a small deviation between data and simulation is present for kaon tracks with momenta less than 0.35 GeV/c. The kaons from ϕ decay in the signal are of low momentum. Consequently, a correction factor of 1.06 for K^+K^- is applied in the detection efficiency, and an uncertainty of 0.5% is assigned for each kaon or pion. The correction factor is the ratio of the efficiencies of data and simulation weighted according to the kaon momentum distribution. We also utilize this control sample to compute the uncertainties associated with PID (0.5%) and π^0 reconstruction efficiency (2.0%) [30].

The uncertainty originating from the ΔE requirement is studied using a control sample of $D^0 \to 2(\pi^+\pi^-)\pi^0$ decays, which has a similar final state as the signal except with a pion pair instead of a kaon pair. The control sample is selected by a relatively loose ΔE requirement, *i.e.*, $\Delta E < 0.1$ GeV, and the corresponding signal yield is extracted by fitting the $M_{\rm BC}$ distribution. The nominal ΔE requirement is then implemented on the control sample, and the resultant ratio of signal yields is taken as the efficiency. The approach is implemented for both data and inclusive MC samples, and the resultant difference in the data and MC efficiencies, 1.4%, is taken as the uncertainty.

The uncertainty from the K^0_S veto is studied by varying the K_S^0 mass window requirement within $\pm 1\sigma$, and the larger difference in the BF, 0.8%, is taken as the uncertainty.

The uncertainties from the MC modeling includes those from the MC statistics (0.8%), $\omega \to \pi^+\pi^-\pi^0$ modeling, quantum correlation (QC) [31] effect, and the longitudinal polarization fraction f_L. The uncertainty due to the $\omega \to \pi^+\pi^-\pi^0$ modeling is assigned to be 0.5% on the basis of two MC samples generated with two different models [32, 33]. From the analysis, the decay $D^0 \to \omega\phi$ appears to be transversely polarized, thus it is a mixture of CP-even and CP-odd components. The uncertainties associated with the polarization is studied by an alternative signal MC sample generated with 1σ upper bound uncertainty, $f_L = 0.10$, and the resultant change in the efficiency, 2.7%, is taken as the uncertainty.

The systematic uncertainty due to the 2D simultaneous fit includes those from signal and background probability density functions (PDFs), the ratio of background between the $M_{\rm BC}$ signal and sideband regions (f), and the fit bias. The uncertainty arising from the signal PDF, 1.2%, is evaluated with an alternative fit, in which the signal PDFs are described using a different non-parameterized modeling of the simulated shape, convolved with a Gaussian function. The uncertainty of the background PDF, 0.4%, is determined by replacing the ARGUS function [26] with a modified one as used in Ref. [27]. The uncertainty from f is 0.1%, evaluated by varying its value within 1 σ when calculating the signal yield. The uncertainty due to the choice of the $M_{\rm BC}$ signal region is evaluated to be 2.7% by enlarging its region by 2 MeV/c^2, which is the resolution of the $M_{\rm BC}$ distribution. The fit bias, 1.0%, is estimated with a large number of pseudo-experiments. Each pseudo-experiment sample is a composition of the signal generated according to the signal PDF and background expectations from the inclusive MC sample. The resultant pull distribution for the BF is consistent with a normal distribution, and we consider the average fit bias as the uncertainty. The uncertainties of $N_{D^0\bar{D}^0}$ and the BFs of the intermediate-state decays are from Ref. [18] and PDG [23], respectively.

The total systematic uncertainty is 5.9% calculated by summing all individual uncertainties quadratically and assuming them to be independent.

The systematic uncertainty for the f_L measurement includes those from MC modeling, $M_{\rm BC}$ signal region, background fraction f, different bin size of $\cos\theta_{\omega,K}$, and signal and background PDFs. We replace the PHSP signal sample with a MC sample generated under the hypothesis of transverse polarization to evaluate the efficiency in each bin of the $\cos\theta_\omega$ and $\cos\theta_K$ distributions. We also extract the signal yields with the alternative $M_{\rm BC}$ signal region, background fraction f, different bin size of $\cos\theta_\omega$ and $\cos\theta_K$, and signal and background PDFs as done for the BF measurement. A joint χ^2 fit is performed to each set of the efficiency corrected signal yields versus $\cos\theta_\omega$ and $\cos\theta_K$ data, and the resultant change in f_L is considered as a systematic uncertainty. Total systematic uncertainty is 0.08 calculated as the quadratic sum of the individual ones.

In summary, the decay $D^0 \to \omega\phi$ is observed for the first time with a significance of 6.3 σ by analyzing the $\psi(3770)$ data taken by the BESIII experiment, corresponding to an integrated luminosity of 2.93 fb^{-1}. The measured BF is $(6.48 \pm 0.96 \pm 0.38) \times 10^{-4}$, which is consistent with the factorization model predictions [1, 7], but inconsistent with predictions based on SU(3) symmetry with nonet symmetry [1], the factorization-assisted topological-amplitude method [8], and the heavy quark effective Lagrangian and chiral perturbation theory [13]. Our angular distribution study reveals that the ω and ϕ in the decay $D^0 \to \omega\phi$ are transversely polarized, which contradicts the prediction from the naïve factorization model [7].

The BESIII collaboration thanks the staff of BEPCII, the IHEP computing center and the supercomputing center of USTC for their strong support. This work is supported in part by National Key Research and Development Program of China under Contracts Nos. 2020YFA0406400, 2020YFA0406300; National Natural Science Foundation of China (NSFC) under Contracts Nos. 11625523, 11635010, 11735014, 11822506, 11835012, 11935015, 11935016, 11935018, 11961141012, 12022510, 12035009, 12035013, 12061131003, 11605196, 11605198, 11705192, 11950410506; 64^{th} batch of Postdoctoral Science Fund Foundation under contract No. 2018M642516; the Chinese Academy of Sciences (CAS) Large-Scale Scientific Facility Program; Joint Large-Scale Scientific Facility Funds of the NSFC and CAS under Contracts Nos. U1732263, U1832207, U1832103, U2032111; CAS Key Research Program of Frontier Sciences under Contract No. QYZDJ-SSW-SLH040; 100 Talents Program of CAS; INPAC and Shanghai Key Laboratory for Particle Physics and Cosmology; ERC under Contract No. 758462; European Union Horizon 2020 research and innovation programme under Contract No. Marie Sklodowska-Curie grant agreement No 894790; German Research Foundation DFG under Contracts Nos. 443159800, Collaborative Research Center CRC 1044, FOR 2359, FOR 2359, GRK 214; Istituto Nazionale di Fisica Nucleare, Italy; Ministry of Development of Turkey under Contract No. DPT2006K-120470; National Science and Technology fund; Olle Engkvist Foundation under Contract No. 200-0605; STFC (United Kingdom); The Knut and Alice Wallenberg Foundation (Sweden) under Contract No. 2016.0157; The Royal Society, UK under Contracts Nos. DH140054, DH160214; The Swedish Research Council; U. S. Department of Energy under Contracts Nos. DE-FG02-05ER41374, DE-SC-0012069.

[1] A. N. Kamal, R.C. Verma, and N. Sinha, Phys. Rev. D **43**, 843 (1991).

[2] P. Bedaque and V. S. Mathur, Phys. Rev. D **49**, 269 (1994).

[3] I. Hinchliffe and T. A. Kaeding, Phys. Rev. D **54**, 914 (1996).

[4] X. W. Kang and H. B. Li, Phys. Lett. B **684**, 137 (2010).

[5] J. Charles, S. D. Genon, X. W. Kang, H. B. Li, and G. R. Lu, Phys. Rev. D **81**, 054032 (2010).

[6] A. F. Falk, Y. Grossman, Z. Ligeti, and A. A. Petrov, Phys. Rev. D **65**, 054034 (2002)

[7] H. Y. Cheng and C. W. Chiang, Phys. Rev. D **81**, 114020 (2010).

[8] H. Y. Jiang, F. S. Yu, Q. Qin, H. N. Li, and C. D Lu, Chin. Phys. C **42**, 063101 (2018).

[9] D. M. Coffman *et al.* (Mark III Collaboration), Phys. Rev. D **45**, 2196 (1992).

[10] E. Hassan, E. Aaoud, and A. N. Kamal, Phys. Rev. D **59**, 114013 (1999).

[11] Y. Amhis *et al.* (Heavy Flavor Averaging Group), arXiv:1909.12524 (2019).

[12] J. M. Link *et al.* (FOCUS Collaboration), Phys. Rev. D **75**, 052003 (2007).

[13] B. Bajc, S. Fajfer, R. J. Oakes, and S. Prelovsek, Phys. Rev. D **56**, 7207 (1997).

[14] H. Albrecht *et al.* (ARGUS Collaboration), Z. Phys. C **64**, 375 (1994).

[15] I. Dunietz, H. Quinn, A. Snyder, and W. Toki, Phys. Rev. D **43**, 2193 (1991).

[16] G. Valencia, Phys. Rev. D **39**, 3339 (1989).

[17] M. Ablikim *et al.* (BESIII Collaboration), Chin. Phys. C **37**, 123001 (2013); Phys. Lett. B **753**, 629 (2016).

[18] M. Ablikim *et al.* (BESIII Collaboration), Chin. Phys. C **42**, 083001 (2018).

[19] M. Ablikim *et al.* (BESIII Collaboration), Nucl. Instrum. Meth. A **614**, 345 (2010).

[20] S. Agostinelli *et al.* (GEANT4 Collaboration), Nucl. Instrum. Meth. A **506**, 250 (2003).

[21] S. Jadach, B. F. L. Ward, and Z. Was, Phys. Rev. D **63**, 113009 (2001).

[22] D. J. Lange, Nucl. Instrum. Meth. A **462**, 152 (2001); R. G. Ping, Chin. Phys. C **32**, 599 (2008).

[23] P. A. Zyla *et al.* (Particle Data Group), Prog. Theor. Exp. Phys. **2020**, 083C01 (2020).

[24] J. C. Chen, G. S. Huang, X. R. Qi, D. H. Zhang, and Y. S. Zhu, Phys. Rev. D **62**, 034003 (2000).

[25] K. S. Cranmer, Comput. Phys. Commun. **136**, 198 (2001).

[26] H. Albrecht *et al.* (ARGUS Collaboration), Phys. Lett. B **241**, 278 (1990).

[27] M. Ablikim *et al.* (BESIII Collaboration), Phys. Rev. D **98**, 032001 (2018).

[28] M. Ablikim *et al.* (BESIII Collaboration), Phys. Rev. Lett. **121**, 171803 (2018).

[29] M. Ablikim *et al.* (BESIII Collaboration), Phys. Rev. Lett. **116**, 082001 (2016).

[30] M. Ablikim *et al.* (BESIII Collaboration), Phys. Rev. D **97**, 072004 (2018).

[31] D. Asner and W. Sun, Phys. Rev. D **73**, 034024 (2006); E: **77**, 019901 (2008).

[32] P. Adlarson *et al.* (WASA-at-COSY Collaboration), Phys. Lett. B **770**, 418 (2017).

[33] M. Ablikim *et al.* (BESIII Collaboration), Phys. Rev. D **98**, 112007 (2018).